

Effects of Two Energy Scales in Weakly Dimerized Antiferromagnetic Quantum Spin Chains

A. Brühl¹, B. Wolf¹, V. Pashchenko¹, M. Anton¹, C. Gross¹, W. Assmus¹, R. Valenti², S. Glocke³, A. Klümper³, T. Saha-Dasgupta⁴, B. Rahaman⁴, and M. Lang¹

¹*Physikalisches Institut, Universität Frankfurt, D-60438 Frankfurt, Germany*

²*Institut für Theoretische Physik, Universität Frankfurt, D-60438 Frankfurt(M), Germany*

³*Theoretische Physik, Universität Wuppertal, 42097 Wuppertal, Germany and*

⁴*S.N. Bose National Centre for Basic Sciences, Salt Lake City, Kolkata 700098, India*

(Dated: June 15, 2021)

By means of thermal expansion and specific heat measurements on the high-pressure phase of $(\text{VO})_2\text{P}_2\text{O}_7$, the effects of two energy scales of the weakly dimerized antiferromagnetic $S = 1/2$ Heisenberg chain are explored. The low energy scale, given by the spin gap Δ , is found to manifest itself in a pronounced thermal expansion anomaly. A quantitative analysis, employing T-DMRG calculations, shows that this feature originates from changes in the magnetic entropy with respect to Δ , $\partial S^m / \partial \Delta$. This term, inaccessible by specific heat, is visible only in the weak-dimerization limit where it reflects peculiarities of the excitation spectrum and its sensitivity to variations in Δ .

PACS numbers: 75.50.Ee, 75.40.Cx, 75.30Et, 75.80.+q, 71.15.Mb, 05.10.Cc

In recent years, many interesting and unexpected effects have been discovered in low-dimensional antiferromagnetic (afm) quantum-spin systems. Prime examples include the Haldane gap for spin $S = 1$ chains, magnetization plateaux in coupled-dimer systems, and the different ground states for even- and odd-leg ladder systems, see, e.g. [1, 2, 3, 4]. These phenomena reflect the intricate many-body quantum character of the systems which renders advanced mathematical methods necessary to gain a quantitative understanding of the experimental observations. In this communication, we want to address another non-trivial collective phenomenon, overlooked in the past, of the effects of two different energy scales caused by a weak alternation in the spin-spin interaction of an $S = 1/2$ afm Heisenberg chain. These scales determine the physical properties of the interacting system at different temperatures. If J_1 and J_2 ($< J_1$) denote the alternating afm coupling constants between nearest neighboring spins along the chain, we define J_1 as the large scale and the spin gap Δ , induced by any amount of alternation [5] $\tilde{\alpha} < 1$ with $\tilde{\alpha} \equiv J_2/J_1$, as the small one. The dominant feature, governing the magnetic and thermodynamic properties at elevated temperatures, is connected with J_1 . In the magnetic susceptibility χ , for example, the maximum due to short-range order is located at $k_B T_\chi^{\text{max}} = 0.64 J_1$, practically independent of $\tilde{\alpha}$ [6]. However as will be shown below, the small energy scale introduces a second distinct anomaly [7], which can be extraordinarily large in the coefficient of thermal expansion. The feature observed here is no longer proportional to that in the specific heat, viz., the so-called Grüneisen-scaling [8] does not apply.

For the study of the effects of two energy scales in the interesting weak-dimerization regime, the high-pressure variant of $(\text{VO})_2\text{P}_2\text{O}_7$ (HP-VOPO) appears particularly well suited. HP-VOPO, first synthesized by Azuma *et*

al. [9], comprises one kind of $S = 1/2$ (V^{4+}) chains with alternating afm Heisenberg interactions [9, 10], as opposed to the ambient-pressure (AP) variant, where two slightly different chain types were identified [10, 11]. No magnetic ordering has been found in HP-VOPO down to 1.5 K $\sim 0.01 J_1/k_B$, the lowest temperature studied so far, indicating that interchain interactions are weak.

To verify that the model of an alternating afm Heisenberg chain is appropriate for HP-VOPO, we carried out *ab initio* density functional (DFT) calculations in the generalized gradient approximation using an LMTO basis. Our analysis of the DFT results in terms of the Nth-order muffin-tin orbital-based downfolding technique [12], shows that the dominant V-V effective hopping integrals are the intrachain hopping via the PO_4 unit, $t_1 = 0.114$ eV, followed by the nearest neighbor V-V intrachain hopping $t_2 = 0.10$ eV. The next non-negligible V-V hopping is along the b -axis, $t_b = 0.02$ eV. Since all other possible V-V interaction paths are more than one order of magnitude smaller than $t_{1,2}$, this analysis clearly confirms the alternating-chain nature of HP-VOPO.

Single crystals of HP-VOPO were prepared by transforming previously grown AP-VOPO crystals under suitable pressure and temperature conditions (3 GPa/800°C) [13]. Structure studies reveal *phase purity* within the experimental resolution of 2-3% and give parameters in accordance with published data [14]. ESR measurements yield a g -factor of $g = 1.977$ for $B \perp c$. The magnetic susceptibility, measured by employing a Quantum Design SQUID magnetometer, is very similar to the results in ref. [10]. A good description of our $\chi(T)$ data for $B \perp c$ at 2-350 K is obtained by using eq. (13a) in ref. [10], the above g -factor, and the following parameters: $J_1/k_B = 127$ K, $J_2/k_B = 111$ K, i.e., $\tilde{\alpha} = 0.873$ and $\Delta/k_B = 31.8$ K, and a concentration of 3.9% of paramagnetic $S = 1/2$ moments per mole V^{4+} with an afm Weiss temperature Θ_W

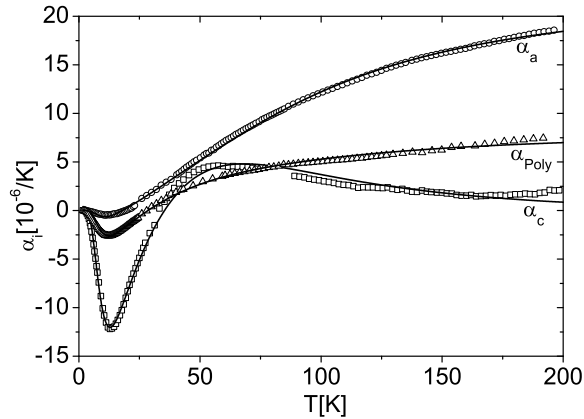


FIG. 1: Expansion coefficients of single-crystalline HP-VOPO along the inter-chain a - (open circles), and intra-chain c -axis (open squares) and for polycrystalline material α_{poly} (open triangles). Solid lines are fits discussed in the text.

$= (2 \pm 0.6)$ K. These parameters, being in good agreement with those given in ref. [10], also provide a consistent description of the specific heat and thermal expansion data, see below, and indicate that impurity effects are of no relevance in the T range discussed here.

The thermal expansion was measured at temperatures 1.5–200 K employing a high-resolution capacitive dilatometer [15]. For the specific heat measurements at 2–30 K, a home-built AC calorimeter [16] was used.

Figure 1 depicts the uniaxial expansivities $\alpha_i(T) = l^{-1}dl/dT$ measured on an HP-VOPO single crystal along ($i = c$) and perpendicular ($i = a$) to the spin-chain direction, together with data for polycrystalline material α_{poly} . In accordance with the crystal structure, the α_i 's are strongly anisotropic. Particularly striking is the anomalous in-chain c -axis expansivity, α_c , yielding a huge negative peak anomaly around 13 K followed by a change of sign and a maximum at 50 K. At elevated temperatures $T \gtrsim 150$ K, α_c becomes very small, indicating an unusually small lattice contribution to α_c . In contrast, α_a and α_{poly} show a much larger lattice expansivity with a small minimum at 13 K and no obvious anomaly at 50 K.

As will be argued below, it is these two distinct features at 50 K and 13 K, dominating the intra-chain expansivity α_c , in which the two energy scales become manifested in HP-VOPO. An indication for the low-energy scale, though much less strongly pronounced, is also visible in the specific heat of HP-VOPO, shown in Fig. 2. The data reveal a weak variation at low temperatures, consistent with a spin gap, and a shoulder-like anomaly around 13 K. The latter feature can be discerned also in the $C(T)$ data on HP-VOPO by Azuma *et al.* [9], where it has been assigned to a Schottky-type anomaly.

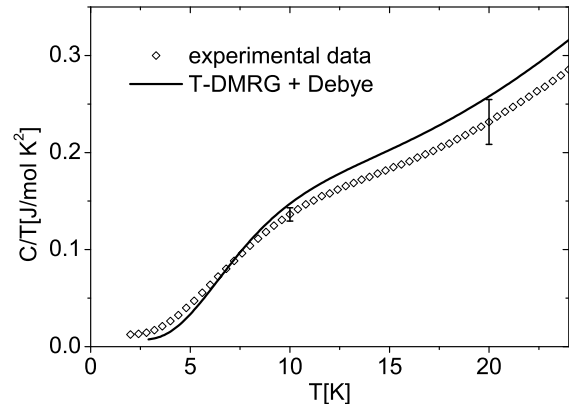


FIG. 2: Specific heat as C/T of single crystalline HP-VOPO (\diamond) of mass $m = 0.74$ mg. Solid line corresponds to model calculations described in the text.

For the description of the magnetic contribution C^m to the specific heat of HP-VOPO in Fig. 2, the density matrix renormalization group approach for transfer matrices (T-DMRG) has been used where the free energy of a one-dimensional quantum system can be calculated by use of the Trotter-Suzuki mapping [17]. For all calculations we have retained between 64 and 100 states and used the Trotter parameter $\epsilon = 0.025$ so that the error of the Trotter-Suzuki mapping is of the order $O(\epsilon^2) \approx 10^{-4}$, whereas the truncation error is of the order 10^{-7} . The phonon background C^{ph} was approximated by a Debye model with a Debye temperature $\Theta_D = 426$ K, which provides a reasonable description of the lattice contribution to the thermal expansion, see below. Instead of fitting the C^m data with J_1 and J_2 as adjustable parameters, requiring extensive computing time, T-DMRG calculations for $J_1/k_B = 127$ K and $J_2/k_B = 111$ K were used. As the solid line in Fig. 2 demonstrates, this ansatz describes the $C(T)$ data reasonably well. Most notably, it proves the hump anomaly in $C(T)$ at low temperatures to be an intrinsic feature of the weakly-dimerized afm $S = 1/2$ Heisenberg chain. The departure of the solid line from the data at higher temperatures is assigned to the inadequacy of the simple Debye model in accurately describing the phonons in this temperature range.

To gain more insight into the nature of the distinct low-temperature anomalies in HP-VOPO, a simplified model, denoted *independent-magnon approximation* (IMA) in the following, will be introduced, see also ref. [6]. The significance of the IMA is verified by comparison with the accurate T-DMRG results. The thermodynamic calculations performed within the IMA are based on a singlet ground state separated by an energy gap Δ from a band of spin-1 excitations, cf. inset to Fig. 3. To restrict the

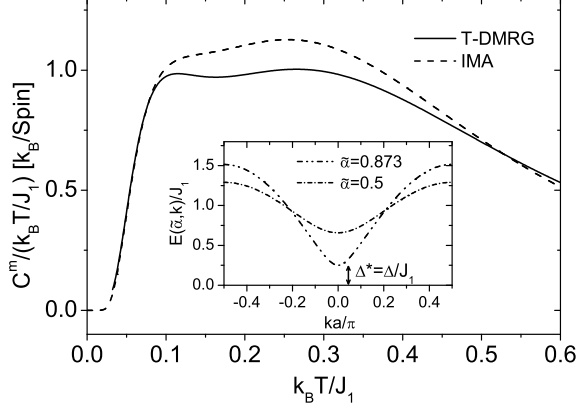


FIG. 3: Magnetic specific heat divided by $k_B T/J_1$ vs. $k_B T/J_1$ for the afm $S = 1/2$ alternating-exchange Heisenberg chain with $J_1/k_B = 127$ K and $J_2/k_B = 111$ K calculated by T-DMRG (solid line) and IMA (broken line). Inset shows one-magnon dispersion relations for the alternation parameter $\tilde{\alpha} = 0.873$ and 0.5 , calculated by using eq. (23a) in ref. [6].

maximum number of excited states to 2^N , with N the number of $S = 1/2$ sites, the occupancy of a one-magnon state with energy $E(k)$ and wave vector k is allowed to be either 0 or 1. In zero field, where the one-magnon band is threefold degenerate, we obtain for the magnetic contribution to the free energy per spin:

$$F^m = -\frac{k_B T d}{2\pi} \int_{-\pi/2d}^{\pi/2d} \ln \left(1 + 3 \exp \left(-\frac{E(\tilde{\alpha}, k)}{k_B T} \right) \right) dk. \quad (1)$$

Here d is the average spin-spin distance along the chains. The one-magnon dispersion $E(\tilde{\alpha}, k)$ was calculated to high accuracy by Barnes *et al.* [19]. A fairly simple parametrization, given by eq. (23a) in ref. [6], is used here for numerical computations of F^m , the magnetic entropy $S^m = -(\partial F^m / \partial T)_V$ and $C^m = -T(\partial^2 F^m / \partial T^2)_V$. Figure 3 compares the so-derived C^m with results from T-DMRG calculations. A representation C/T is chosen to make the low-temperature anomaly clearer. As expected, the IMA nicely traces the T-DMRG results at low temperatures, where the magnon density is small. In particular, it shows the peak anomaly in C^m/T at $k_B T/J_1 \sim 0.1$, a signature of the low-energy scale. For temperatures $0.06 \leq k_B T/J_1 \leq 0.5$, however, the IMA tends to overestimate C^m by about 10% at maximum. The accompanied extra entropy is balanced at higher temperatures, so that at $k_B T = 2J_1$ (not shown), both models reveal about 97 % of the full spin entropy.

With these models at hand, a detailed description of the anomalous thermal expansion of HP-VOPO is possible. If the entropy of a system can be expressed as

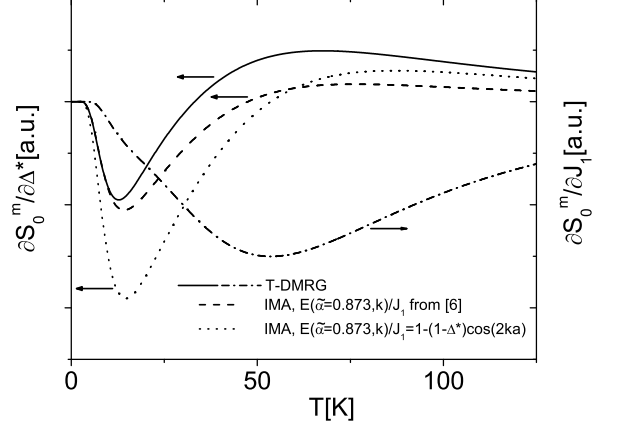


FIG. 4: Temperature dependence of (i) $\partial S_0^m / \partial \Delta^*$ (left scale) and (ii) $\partial S_0^m / \partial J_1$ (right scale) for the alternating afm $S = 1/2$ Heisenberg chain with $J_1/k_B = 127$ K and $J_2/k_B = 111$ K, i.e. $\tilde{\alpha} = 0.873$ and $\Delta/k_B = 31.8$ K. While for (i) T-DMRG results are compared with IMA results for different dispersion relations given in the figure, (ii) is calculated within T-DMRG.

a sum of separate contributions $S = \sum_j S^j$, the volume expansion coefficient can be written as [8] $\beta = \sum_j \beta^j = \kappa_T \sum_j (\partial S^j / \partial V)_T$, with $\kappa_T = -V^{-1}(\partial V / \partial P)_T$ the isothermal compressibility. This holds true also for anisotropic systems as long as the volume changes occur under hydrostatic conditions [8]. For HP-VOPO, the sum j runs over the magnetic ($j = m$) and phonon (ph) contributions. The use of the Debye model and the *scale invariance* of S^m imply that $S = S^{ph}(T/\Theta_D) + S^m(T/J_1, \Delta^*)$, where $\Delta^* = \Delta/J_1$. With $C_0^{ph} = -\Theta_D \partial S_0^{ph} / \partial \Theta_D$ and $C_0^m = -J_1 \partial S_0^m / \partial J_1$, the phonon and magnetic molar specific heat contributions, respectively, one finds

$$\beta = \frac{\kappa_T}{V_0} (-\Delta^* \Gamma^{\Delta^*} \frac{\partial S_0^m}{\partial \Delta^*} + \Gamma^{J_1} C_0^m + \Gamma^{ph} C_0^{ph}). \quad (2)$$

Here $\Gamma^{\Delta^*} = -\partial \ln \Delta^* / \partial \ln V$, $\Gamma^{J_1} = -\partial \ln J_1 / \partial \ln V$ and $\Gamma^{ph} = -\partial \ln \Theta_D / \partial \ln V$ define different Grüneisen parameters which measure the volume dependence of the respective characteristic temperature or energy. Note that as a consequence of S^m being a function of the two scaling variables T/J_1 and Δ^* , β (eq. 2) contains a contribution $\propto \partial S_0^m / \partial \Delta^*$, which has no counterpart in the magnetic specific heat, i.e., β^m is no longer proportional to C^m , viz. Grüneisen-scaling does not apply.

Equation 2 can be generalized to the uniaxial expansivities by $\alpha_i = \gamma_i^{\Delta^*} \partial S_0^m / \partial \Delta^* + \gamma_i^{J_1} \partial S_0^m / \partial J_1 + \gamma_i^{ph} \partial S_0^{ph} / \partial \Theta_D$, $i = a, b, c$. The prefactors $\gamma_i^{\Delta^*}$, $\gamma_i^{J_1}$ and γ_i^{ph} contain the respective strain dependencies of Δ^* , J_1 and Θ_D , some combinations of elastic compliances and

the molar volume V_0 , see [8]. Since these quantities, along with the Grüneisen parameters Γ^J in eq. (2), generally reveal only a very weak variation with temperature, they can be treated as constants [20]. In leading order, the T dependence of α_i and β is thus given by the derivatives of the entropy with respect to the different energy scales.

The two magnetic terms of interest here, computed numerically within the IMA (eq. (1)) and T-DMRG for $J_1/k_B = 127$ K and $J_2/k_B = 111$ K, are displayed in Fig. 4 as a function of temperature. For $\partial S_0^m/\partial J_1 (= -C_0^m/J_1)$, a broad anomaly is revealed around 50 K, reflecting the short-range afm correlations associated with J_1 . In addition, $\partial S_0^m/\partial J_1$ discloses a tiny feature around 13 K, corresponding to the low-temperature maximum in $C^m/T = -J_1/T \cdot \partial S_0^m/\partial J_1$ in Fig. 3, as a result of the gap formation. Since this anomaly is much smaller and has the same sign as the one at 50 K, it cannot account for the change in sign and the large negative peak anomaly in α_c at 13 K. However, as shown in Fig. 4, such an anomaly is revealed by $\partial S_0^m/\partial \Delta^*$. This feature, constituting the central result of this paper, reflects the sensitivity of the magnetic entropy to changes in the spin gap Δ , probed in a most sensitive differential way by the expansivity. The effect can be observed only in the weak-dimerization limit, where the energy scales are clearly separated. Here the minimum in the one-magnon dispersion is narrow so that the magnetic excitation spectrum is very susceptible to small changes in Δ , cf. inset to Fig. 3. To simulate the effect of such changes on the expansivity, comparative calculations of $\partial S_0^m/\partial \Delta^*$ have been performed within the IMA using different dispersion relations $E(\tilde{\alpha}, k)$ delimiting the spectrum to low energies, cf. Fig. 4. While for $E(\tilde{\alpha} = 0.873, k)$ shown in the inset to Fig. 3, the calculations within the IMA (broken line in Fig. 4) nicely reproduce the T-DMRG results (solid line) up to the minimum position, a gapped $\cos(2ka)$ dispersion with the same gap value gives rise to an anomaly in $\partial S_0^m/\partial \Delta^*$ (dotted line) which markedly deviates from the T-DMRG data. These results highlight the extraordinarily high sensitivity of the expansivity to peculiarities of the magnetic excitation spectrum associated with the low energy scale.

Employing the prefactors $\gamma_i^{J_1}$, $\gamma_i^{\Delta^*}$ and γ_i^{ph} and Θ_D as adjustable parameters, the expression for the uniaxial expansivities can be used to fit the α_a and α_c data in Fig. 1 (solid lines). The good quality of the fit to α_a for $T \gtrsim 70$ K, where the phonon contribution dominates, validates the use of the Debye model with $\Theta_D = 426$ K for satisfactorily describing the phonons in HP-VOPO. The lattice contribution, however, plays a minor role for α_c . Here an excellent fit is obtained essentially by the superposition of the two magnetic contributions depicted in Fig. 4, properly scaled by $\gamma_c^{J_1}$ and $\gamma_c^{\Delta^*}$. After having assured the validity of our ansatz through these fits to α_c and α_a , a modeling of the volume expansivity $\beta = \alpha_a + \alpha_b + \alpha_c$ is possible by means of eq. (2), cf. solid line through $\alpha_{poly} = \beta/3$ in Fig. 1. Employing a rough

estimate for the bulk modulus of $c_B = \kappa_T^{-1} = (47 \pm 6)$ GPa from $\Theta_D = 426$ K [22], the fit yields the following Grüneisen parameters $\Gamma^{\Delta^*} = -45 \pm 6$, $\Gamma^{J_1} = 1.3 \pm 0.2$ and $\Gamma^{ph} = 0.3 \pm 0.1$. Particularly striking is the large $\Gamma^{\Delta} = \Gamma^{\Delta^*} + \Gamma^{J_1} \simeq -43 \pm 6$, reflecting a huge pressure dependence of the spin gap $\partial \Delta/\partial P = \Delta \cdot \kappa_T \cdot \Gamma^{\Delta} = -(28 \pm 8)$ K/GPa. A linear extrapolation to finite pressure implies that hydrostatic pressure of about (1.1 ± 0.3) GPa is sufficient to close the spin gap in HP-VOPO, i.e. to drive the system to the quantum critical uniform limit.

In summary, the high-pressure variant of $(\text{VO})_2\text{P}_2\text{O}_7$ has been used to study the effects of two distinct energy scales of the afm $S = 1/2$ weakly-dimerized Heisenberg chain. We show that $\partial S_0^m/\partial J_1$ accounts for the signatures in the specific heat associated with short-range afm correlations and spin-gap formation. However, this term cannot explain the large low-temperature anomaly observed in the intra-chain expansivity. The latter feature is well described by $\partial S_0^m/\partial \Delta^*$, which probes the entropy contours with respect to changes in the spin gap. This term, inaccessible by specific heat, is observable only in the weak-dimerization limit and reflects the high sensitivity of the excitation spectrum, as regards small changes in Δ . Our results, which are based on the scale invariance of the entropy $S^m(J_1, J_2, T) = S^m(T/J_1, J_2/J_1)$, can be generalized to cover the large family of magnetic multi-scale systems described by Heisenberg-like models.

The authors acknowledge fruitful discussions with B. Lüthi. The T-DMRG calculations have been supported by the DFG under contracts No. KL645/4-2 and GK1052.

-
- [1] F.D.M. Haldane, Phys. Rev. Lett. **50**, 1153 (1983).
 - [2] I. Affleck, J. Condens. Matter **1**, 3047 (1989).
 - [3] E. Dagotto and T.M. Rice, Science **271**, 618 (1996).
 - [4] M. Oshikawa *et al.*, Phys. Rev. Lett. **78**, 1984 (1997).
 - [5] J.C. Bonner *et al.*, J. Appl. Phys. **50**, 1810 (1979).
 - [6] D.C. Johnston *et al.*, Phys. Rev. B **61**, 9558 (2000).
 - [7] An anomaly can also be discerned in $\chi(T)$ calculated by various techniques, provided $\tilde{\alpha} \gtrsim 0.8$ [6].
 - [8] T.H. Barron *et al.*, Adv. in Phys. **29**, 609 (1980).
 - [9] A. Azuma *et al.*, Phys. Rev. B **60**, 101454 (1999).
 - [10] D.C. Johnston *et al.*, Phys. Rev. B **64**, 134403 (2001).
 - [11] A.W. Garrett *et al.*, Phys. Rev. Lett. **79**, 745 (1997).
 - [12] O.K. Andersen and T. Saha-Dasgupta, Phys. Rev. B **62**, R16219 (2000), and references therein.
 - [13] C. Gross *et al.*, High Pressure Research **22**, 581 (2002).
 - [14] T. Saito *et al.*, J. Solid State Chemistry **153**, 124 (2000).
 - [15] R. Pott *et al.*, J. Phys. E **16**, 444 (1983).
 - [16] J. Müller *et al.*, Phys. Rev. B **65**, R140509 (2002).
 - [17] J. Sirker, A. Klümper, Europhys. Lett. **60**, 262 (2002).
 - [18] T. Barnes, Phys. Rev. B **67**, 024412 (2003).
 - [19] T. Barnes *et al.*, Phys. Rev. B **59**, 11384 (1999).
 - [20] This is no longer valid close to the quantum critical point ($\Delta \rightarrow 0$), where the Grüneisen parameter diverges [21].
 - [21] L. Zhu *et al.*, Phys. Rev. Lett. **91**, 066404 (2003).
 - [22] This is possible within an isotropic approximation, see

G.A. Alers in *Physical Acoustics*, Academic Press (1965).